



Field Surveys and Numerical Simulation of the 2018 Typhoon Jebi: Impact of High Waves and Storm Surge in Semi-enclosed Osaka Bay, Japan

TUAN ANH LE,¹  HIROSHI TAKAGI,¹ MOHAMMAD HEIDARZADEH,² YOSHIHUMI TAKATA,¹ and ATSUHEI TAKAHASHI¹

Abstract—Typhoon Jebi made landfall in Japan in 2018 and hit Osaka Bay on September 4, causing severe damage to Kansai area, Japan's second largest economical region. We conducted field surveys around the Osaka Bay including the cities of Osaka, Wakayama, Tokushima, Hyogo, and the island of Awaji-shima to evaluate the situation of these areas immediately after Typhoon Jebi struck. Jebi generated high waves over large areas in these regions, and many coasts were substantially damaged by the combined impact of high waves and storm surges. The Jebi storm surge was the highest in the recorded history of Osaka. We used a storm surge–wave coupled model to investigate the impact caused by Jebi. The simulated surge level was validated with real data acquired from three tidal stations, while the wave simulation results were verified with observed data from four wave monitoring stations. The high accuracy of the model demonstrates the usefulness of numerical simulations to estimate the heights of storm surges and wind waves at specific locations, especially where no monitoring stations are available. According to the simulation, the significant wave height was nearly 13 m in the entrance of Kii Strait between Tokushima and Wakayama and 4 m inside Osaka Bay. During the field survey, we encountered collapsed sea dykes, which were obviously damaged by high waves. In fact, the storm surge reached only 1.7 m above the normal tidal level at Kobe, Hyogo, which was not extremely high. Hence, the combination of storm surge and high waves can explain the extent of destruction in Hyogo, such as the failure of an inland floodgate and a stranded large vessel over the breakwater, which were observed during the field survey. We emphasize the importance of adequate coastal designs against high waves even in semi-enclosed bays, as they seem to have been underestimated when the typhoon disaster risk management was conducted.

Key words: Typhoon Jebi, high wave, storm surge, field survey, Kansai, Japan, numerical simulation.

1. Introduction

Annually, an average of 2.9 tropical cyclones (from 1951 to 2016) have hit Japan (Takagi and Esteban 2016; Takagi et al. 2017). The recent Typhoon Jebi in September 2018 has been the strongest tropical cyclone to come ashore in the last 25 years since Typhoon Yancy (the 13th typhoon to hit Japan, in 1993), severely damaging areas in its trajectory.

Tropical cyclones are very hazardous and extreme meteorological phenomena affecting most coastal countries worldwide. In fact, strong winds and heavy rainfall from tropical cyclone landfall can cause major disasters. Among others, storm surge can have the most life-threatening impact during the course of a major storm.

For example, Hurricane Katrina in 2005 caused over 1000 fatalities in Louisiana and 200 in Mississippi due to the storm surge that exceeded 10 m in several locations along the Mississippi coastline (Fritz et al. 2007). Likewise, Typhoon Haiyan caused enormous damage to the Philippines in 2013, with more than 6000 reported death (NDRRMC 2014), given the storm surge reached over 6 m in the innermost part of Leyte Gulf (Mikami et al. 2016; Takagi et al. 2016). Although the number of casualty was relatively low, Typhoon Hato in 2017 generated about 2.5-m storm surge in Macau and significantly impacted Macau's economy, especially regarding the casino industry (Takagi et al. 2018).

Strong winds during the course of a typhoon can also generate high waves, which may cause the predominant physical impact. The maximum hindcast wave heights during the passage of Typhoon Haiyan reached 20 m at eastern Samar (Bricker et al. 2014).

¹ School of Environment and Society, Tokyo Institute of Technology, 2-12-1 Ookayama, Meguro-ku, Tokyo 152-8550, Japan. E-mail: letuananh.aa@m.titech.ac.jp; takagi@ide.titech.ac.jp; takata.y.ab@m.titech.ac.jp; takahashi.a.as@m.titech.ac.jp

² Department of Civil and Environmental Engineering, Brunel University London, Uxbridge UB8 3PH, UK. E-mail: Mohammad.Heidarzadeh@brunel.ac.uk

In addition, Roeber and Bricker (2015) investigated the destructive tsunami-like wave that devastated the town of Hernani, Eastern Samar, the Philippines during Haiyan.

Typhoon Jebi was the fourth to hit Japan in the 2018 season, notably affecting Kansai area, Japan's second biggest, populous, and prosperous region, which is prone to typhoons and storm surges. Jebi caused 13 deaths and 741 injured people as of September 14, 2018 (Fire and Disaster Management Agency 2018). Furthermore, power outages occurred in the wider region of Kansai, affecting approximately 2.2 million residencies. The bridge connecting Kansai International Airport to mainland Japan was damaged following the collision of a large freighter, which was stranded due to the rough sea state caused by Typhoon Jebi. Thus transportation was interrupted to this, the largest international airport in western Japan, located on an artificial island in Osaka Bay. Moreover, Kansai International Airport was severely flooded during Typhoon Jebi, and around 5000 people were forced to remain at the airport overnight.

A wind radius of 50-kt was estimated around 220 km (in the longest axis) when Jebi was about to make landfall (Fig. 1). Jebi maintained maximum wind speed of 75–85 kt (139–157 km/h) when it hit Osaka. The sea level pressure during the passage of Jebi over Osaka Bay was of 950–975 hPa. As Typhoon Jebi swept through the Osaka Bay and the south of Honshu Island, it caused heavy rainfall, high

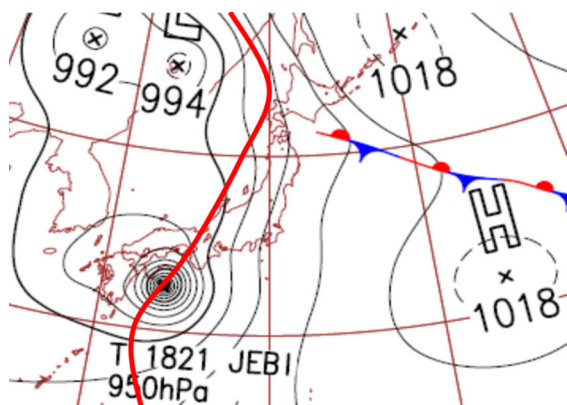


Figure 1

Japan Meteorological Agency's weather map immediately before Jebi made landfall (September 4, 2018, 09:00, Japan Standard Time, UTC + 9) (The red line is Jebi track)

waves, and storm surges. Regarding increase in water level during the typhoon, the highest tidal level in Osaka reached 3.29 m above the mean sea level, exceeding the previous record of 2.93 m during Typhoon Nancy in 1961, according to data from JMA (Japan Meteorological Agency) (Japan Meteorological Agency 2018). In addition, strong winds from the typhoon disrupted cities in the Kansai region, including Osaka, Kyoto, and Kobe. In Kyoto, part of the glass roof over the main rail station collapsed, causing several injuries, according to Japan Times News (2018). The strong winds also damaged infrastructure in downtown Osaka and adjacent cities, where roofs were blown away and vehicles overturned, as evidenced from videos recorded by local people. Floods at coastal residences in Kobe and adjacent cities were also investigated and reported by a Japanese survey team (Takabatake et al. 2018), with reported depths of 0.18–1.27 m caused by the typhoon. Furthermore, many shipping containers were displaced by the storm surge and waves in Ashiya city. Overall, the JMA reported that Typhoon Jebi caused the highest storm surges above the mean sea level ever reported at Osaka (3.3 m), Kobe (2.3 m), Gobo (3.2 m), Shirahama (1.6 m), Kushimoto (1.7 m), and Awayuki (2.0 m).

We carried out a reconnaissance survey 2 days after Typhoon Jebi in the affected area and observed many damaged structures and inundations that were apparently caused by the high waves combined with storm surges. The combination of these two phenomena may have exacerbated the damage in the coasts and even in the innermost part of Osaka Bay. However, no comprehensive study has been conducted to reveal the combined impact of this destructive typhoon to date. This paper reports the situation that we observed during the field survey. The hindcast analysis is also reported to describe the spatial distribution of high waves and storm surge during Jebi. In addition, we present the analysis of tide data provided by the JMA to investigate the significance of storm surges generated by Typhoon Jebi. Based on these observations, we emphasize the importance of adequate coastal designs against high waves, because the associated disaster risk appears to have been underestimated regarding plausible storm

surges occurring in semi-closed bays such as Osaka Bay.

2. Methodology

2.1. Field Survey

We conducted field surveys for 3 days from September 6 to 8, 2018, a few days after Typhoon Jebi made landfall at the Tokushima Prefecture around the noon of September 4. The survey aimed at identifying the damage extent in the typhoon aftermath around the bay of Kansai area including parts of Shikoku Island and Awaji-shima Island (Fig. 2). Laser range finders (TruPulse 360; Laser Technology, Inc.) were used for determining the distance and the elevation of the broken dykes or fences, debris, fallen trees and remaining water mark.

In addition, real-time kinematic GPS receivers (ProMark 100; Ashtech, Inc.) provided ground elevation, and trained staff used handheld GPS receivers (GPSMAP; Garmin Ltd.) to collect the coordinates at the survey points. Checking the abovementioned physical evidence provided information about flooding, wave height, and damage extent at each location (with reference to the local sea level at the time of the survey). When a sign of wave overtopping was observed but no visible water mark or damage was available, the height of protection infrastructure was considered to estimate the wave height. However, the actual wave height should have been larger than the estimated height. The retrieved heights of protection infrastructure, inundation depth, and ground elevation acquired through the laser range finders were corrected to the tidal height above the sea level at the time of the survey by using data from the nearest tidal

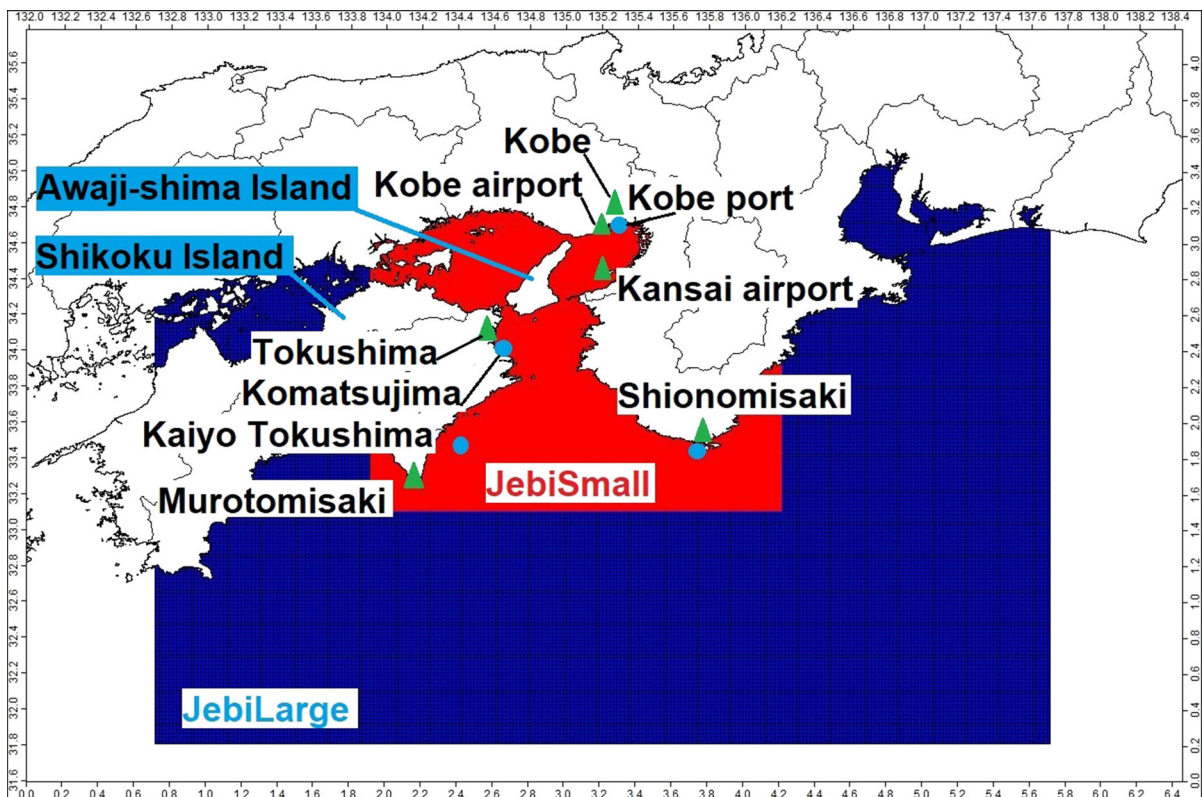


Figure 2

Simulation domains for simulating wind waves during Typhoon Jebi. The indicated locations have wave monitoring stations of the NOWPHAS and wind observation stations from JMA, whose data were used in this study for model verification (circle, wave monitoring station; triangle, wind monitoring station)

station. Furthermore, these data were adjusted from the mean water level in Tokyo Bay (TP) as common reference level. The elevations measured using the GPS receivers were corrected to TP by calibrating with the survey control points provided by the Geospatial Information Authority of Japan (Tsuji et al. 2013).

2.2. Wind–Wave and Storm Surge Hindcasting

There is a two-way interaction between storm surges and waves. Wave height is limited by wave breaking, and waves can also be affected by the increase in total water depth caused by a storm surge, wave setup, and tide. On the other hand, radiation stresses generated by the presence of waves increase the peak water level due to wave setup (Longuet-Higgins and Stewart 1960, 1962). Xie et al. (2008) applied Princeton Ocean Model and Simulating Waves Nearshore (SWAN) model and confirmed the contribution of wave setup to inundation predictions in Charleston Harbor during the 1989 Hurricane Hugo. Funakoshi et al. (2008) applied a coupled model known as ADCIRC (Advanced Circulation Model) and SWAN, finding that wave-induced radiation stresses contributed 10–15% increase in peak water levels during Hurricane Floyd in 1999. Chen et al. (2008) found that the local wind forcing was responsible for 80% of the maximum surge, while the combined effects of tides, surface waves, and offshore surge accounted for the remaining 20% during Hurricane Katrina in 2005.

In this study, waves were simulated using the Delft3D-WAVE module, which uses the SWAN spectral wave model. SWAN is a third-generation wave model to compute random, short-crested, and wind-generated waves in coastal regions and inland waters (Booij et al. 1999). We coded the SWAN model based on the action balance equation with sources and sinks and provided a nesting application to the parent grid. To investigate the influence of this depth-limited condition on wave height, we used the hydrodynamics module Delft3D-FLOW to simulate the combined impact of wave and storm surge. FLOW solves the Navier–Stokes equations for an incompressible fluid under shallow water and Boussinesq's assumptions. Although the Delft3D FLOW

module can be applied to three-dimensional phenomena, we used a two-dimensional horizontal grid, establishing a shallow-water wave model, which is commonly used to simulate long waves such as storm surges, tsunamis, and tidal propagation (Takagi et al, 2019). Delft3D-FLOW is coupled with Delft3D-WAVE through a dynamic interaction, in which the hydrodynamic module receives radiation stresses calculated by the wave module, while the wave module updates the water depth according to the storm surge with the input from the FLOW module. Current feedback was not considered in this study.

The wave simulation was performed by nesting two computational domains. Domain *JebiLarge* (Fig. 2) covers the deep sea outside Japan mainland as parent grid with resolution of $0.02^\circ \times 0.02^\circ$, being used for both hydrodynamic and wave models, whereas domain *JebiSmall* (Fig. 2) includes the inner bay stretch from the Kii Strait to Osaka Bay as nested internal grid with resolution of approximately $500 \text{ m} \times 500 \text{ m}$, being used for detailed wave simulation. The bathymetric data at 500 m intervals and retrieved from the Japan Oceanographic Data Center (JODC) (<http://www.jodc.go.jp/jodcweb/>) was used for both Delft3D-FLOW and Delft3D-WAVE model simulations to incorporate the detailed bathymetry from the study areas. Both models relied on wind fields from the hourly grid point values (GPVs) of numerical weather prediction based on the mesoscale spectral model of the JMA. The forecasting of the mesoscale spectral model is known as the JMA nonhydrostatic model (Saito et al. 2006). The forecast domain is the rectangular area including the entire Japan territory and surrounding area with approximate grid spacing of 5 km (a grid resolution of $0.065^\circ \times 0.05^\circ$ covers the domain from 120°E to 150°E and from 22.4°N to 47.6°N). Data of GPVs are available from the server of the numerical weather prediction/observation data of the JMA (Japan Meteorological Agency. The numerical forecast data/observed data). The data contain many variables including sea-level pressure, surface pressure, and eastward/northward components of wind.

Among the many physical processes available in the Delft3D-WAVE module, we considered depth-induced wave breaking, bottom friction, wind-wave growth, white-capping, nonlinear triad, and

quadruplet interactions for the wave simulation. The wave frequencies for simulations of the Jebi wave were set to from 0.05 to 1 Hz and divided into 24 bins, while the wave directions were divided into 36 bins separated by 10° for each bin. The Delft3D-FLOW model was calculated over the same period of the WAVE model with short timesteps of 0.1 min to obtain stable computational results. The Manning's value was set to $n = 0.02$ as sea-bed roughness. The coupling timestep between the two models was every 20 min. The simulated period for the coupled model started on August 30 at 00:00 and finished on September 5 at 00:00 (UTC) of 2018. Both the FLOW and WAVE models were evaluated for two cases: coupled mode, which considers the wave–flow interaction, and uncoupled mode, where mutual feedback is completely removed. Wind and sea-surface pressure were assigned as external forces in both cases, whereas wave radiation stresses were only used for the coupled mode.

The observed wave data at nearshore stations and offshore buoys during Typhoon Jebi were used to verify the simulation results from Delft3D-WAVE and obtained from the Nationwide Ocean Wave Information Network for Ports and Harbors (NOW-PHAS), which tracks the significant wave height and wave period every 20 min. On the other hand, the measured water level collected from tide gauges along the coastline was provided by Hydrographic and Oceanographic Department managed by the Japan Coast Guard and JMA. These data were used for comparison with the estimated surge level from the Delft3D-FLOW model. The scarcity of wave data makes the results from the numerical model beneficial to estimate the maximum significant wave height and map its spatial distribution over Osaka Bay in Kansai area.

2.3. Analysis of Tide Gauge Data

We analyzed the sea level data at 12 tide gauge stations along the trajectory of Typhoon Jebi (Fig. 3). The original data were sampled at intervals of 15 s and provided by the JMA. Tidal signals were estimated using the MATLAB Tidal Fitting Toolbox (Grinsted 2008), and sea level references were removed to produce detided waveforms. In addition, we applied a 15 min

moving average window to remove wave oscillations (Heidarzadeh et al. 2018). Therefore, by removing the effects of tides and waves, we obtained storm surge levels at each tide gauge station (Fig. 3), from which the surge amplitude (SA) and surge duration (SD) were calculated. The SA is defined as the amplitude difference between the normal sea level elevation and the maximum surge level, whereas SD is the corresponding period during which the sea level is above normal.

A Fourier analysis was also applied to investigate the frequency characteristics in the water level data at selected locations. The conventional fast Fourier transform (Cooley–Turkey algorithm) was applied to derive the power spectrum of component waves. This analysis enabled us to roughly determine whether water level increases primarily by storm surges or wind waves.

3. Results

3.1. Field Survey

Fifteen locations along the coastline of the four most affected prefectures, namely, Osaka, Wakayama, Tokushima, and Hyogo (including Awaji-shima island) were surveyed (Fig. 4, Table 1). Evidence of storm surges, damage of coastal protection, and overtopping induced by high waves were observed. Figure 4 shows the field survey locations with the corresponding storm surge and wave overtopping heights. Although the total water level should have been determined by the combination of waves and storm surge, Fig. 4 distinguishes the primary mechanism for elevated sea level as being either wave overtopping or storm surge based on our onsite observations.

3.1.1 Locations (a) and (b): Osaka Nanko Bird Sanctuary and Sakai

Typhoon Jebi caused the highest storm surge recorded in Osaka Bay. The center of the typhoon crossed along the west side of the bay, and strong winds with a low-pressure system generated severe storm surges particularly at the eastern part of the bay.

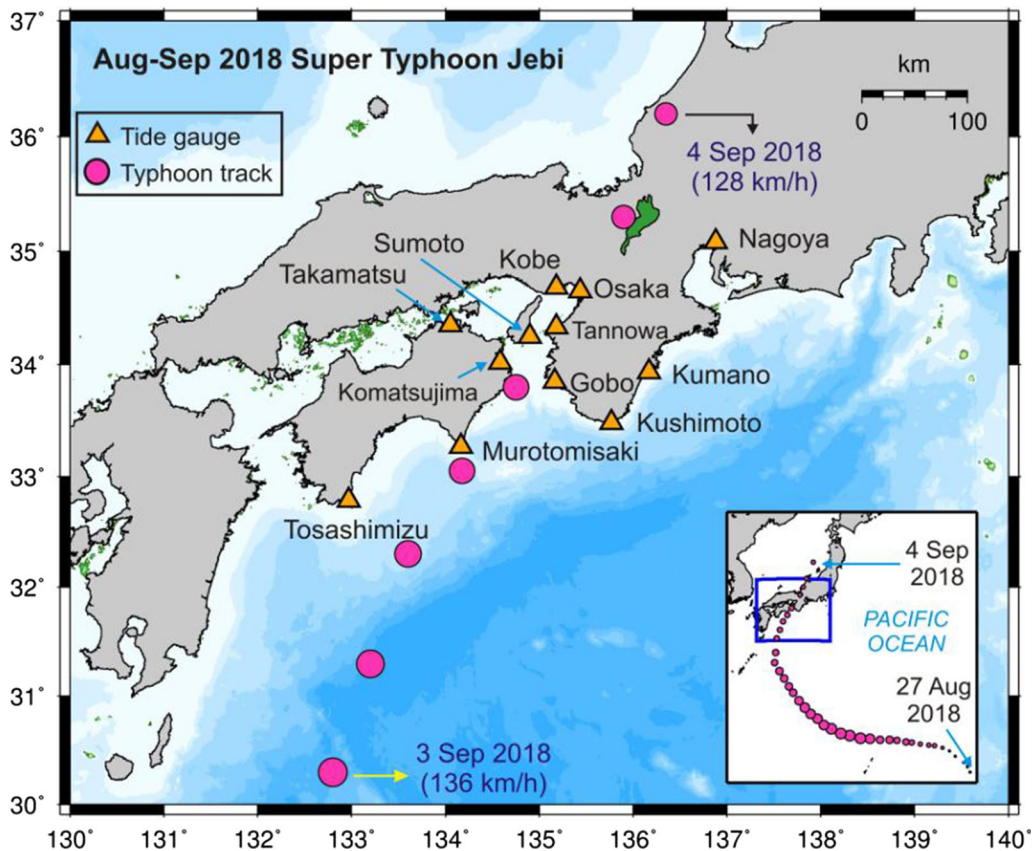


Figure 3

Map of west Japan showing the locations of tide gauge stations (orange triangles) considered in this study and trajectory (pink circles) of Typhoon Jebi from August to September of 2018

The Nanko Bird Sanctuary is located at the northwest corner of Sakishima artificial island in Osaka Bay and is a stopover for migrating birds on their way from the Arctic Circle to Southeast Asia to avoid winter (Fig. 5I). A broken statue surrounded by several fallen tree branches was observed at the main entrance, and many cracked big trees obstructed the main route. The soil was still wet and slippery due to the coastal flooding. Trash was gathered by the wind and floodwater (Fig. 5II). We started to investigate the site immediately behind the seashore, where a dyke with tetrapod blocks was constructed (Fig. 5III). Severe scour behind the dyke was observed (Fig. 5IV). Hence, waves should have overtopped the dyke with a height of 4.05 m relative to TP. Likewise, strong winds should have caused partial damage to the building next to the sea, evidenced by

the broken metal fence and broken windows (Fig. 5V). We measured the elevation from the sea surface to the place where a watermark evidencing the inundation height remained, as we found an obvious visible line distinguishing the inundation on a grassy hill (Fig. 5VI). We observed small white flowers on top of the hill, whereas grass had withered and disappeared (brown color ground can be seen at that place) below the line where seawater had likely reached. Given that this line was almost horizontal, seawater should have been brought by storm surge, whose height relative to TP was estimated to be approximately 3.55 m. At Sakai, the port/industrial city located at the south of Osaka, several sections of coastal dykes with a-2 m high parapet were torn apart most likely due to impressively high wave pressures (Fig. 5VII).

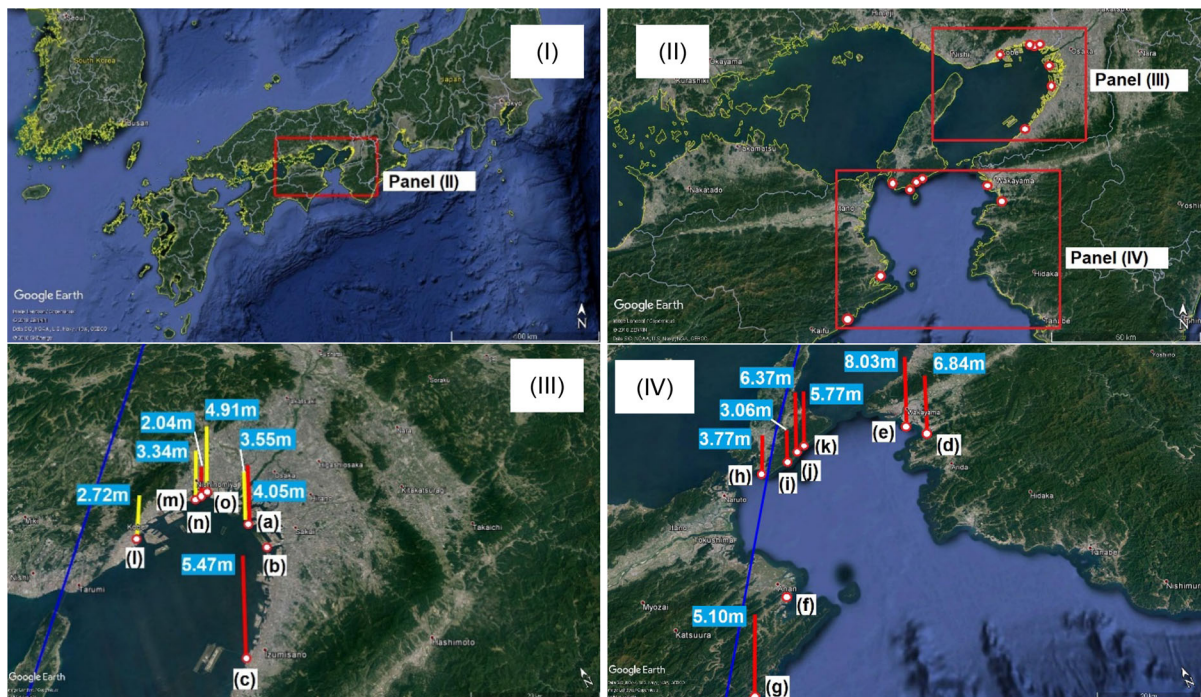


Figure 4

I Large view of field survey area, II location of survey points, III storm surge and overtopping height measurements inside Osaka Bay and IV around Kii Strait. Primary mechanism of elevated sea level: wave overtopping (red) and storm surge (yellow). The blue line indicates the trajectory of Typhoon Jebi. Locations (a–o) indicate the sequence of survey points

3.1.2 Location (c): Osaka Rinku Park

We conducted a survey at the Rinku Park located on the opposite side of Kansai International Airport (Fig. 6). The Rinku Park attracts tourists who arrive from the airport and local people by its greenery, seaside seeing spots, and long walking trails. However, Typhoon Jebi severely damaged the park, and the access for visitors was suspended. When we visited the park 2 days after Jebi, several fallen tree branches remained on the ground near the entrance. Trash was scattered everywhere, though no visible damage to the park infrastructure was observed, except for a roof damage caused by strong winds (the roof cover panels were blown away) (Fig. 6I). No residences are located around the park area. The inundation height was evidenced by the remaining trash on the artificial beach of the park. We measured the elevation from the sea level at the time of our survey to the highest line of visible trash (Fig. 6II),

estimating an inundation height of 5.47 m relative to TP. The park was well protected from the sea by a two-layer infrastructure comprising an outer thick tetrapod layer and an inner large stone barrier. Both layers did not suffer any considerable damage showing that the wave force was not significantly strong, and only wave overtopping caused inundation (Fig. 6II, III). The elevation of the stone dyke is about 1.8 m above the mean sea level.

3.1.3 Locations (d) and (e): Kainan, and Saikazaki in Wakayama Prefecture

Kainan and Saikazaki are located at the northwest coast of the Wakayama Prefecture (Fig. 7I). We found no clear evidence of extensive inundation induced by storm surges in the typhoon aftermath. However, damage caused by wave overtopping were observed at many locations. At Kainan, we visited an entertainment park (Wakayama Marina City), and all

Table 1
Field survey storm surge/wave runup measurements in west Japan due to Typhoon Jebi

No	Location	Latitude (°N)	Longitude (°E)	Date (m/d/yyyy)	Time (Japan standard time) (hh:mm:ss)	Measured height from TP (m)	Observations
(a)	Osaka Nanko Bird Sanctuary	34°38'17.1"	135°23'54.8"	9/6/2018	13:40:00	4.05	Dyke height
	Osaka, Nanko Bird Field	34°38'15.9"	135°24'6.9"	9/6/2018	13:40:00	3.55	Debris
(b)	Osaka, Sakai	34°33'50.6"	135°24'45.1"	9/6/2018	15:22:00	3.25	Ground altitude
(c)	Osaka, Rinku park	34°24'40.5"	135°17'35.9"	9/6/2018	17:22:00	5.47	Debris
(d)	Wakayama, Kainan	34°9'4.9"	135°10'47"	9/7/2018	08:45:00	6.84	Smashed fence
(e)	Wakayama, Saikazaki	34°11'40.9"	135°8'22.2"	9/7/2018	09:54:00	8.03	Smashed parapet
(f)	Tokushima, Anan	33°53'7.1"	134°40'8.9"	9/7/2018	13:00:00	–	House with damaged roof
(g)	Tokushima, Minami Town	33°43'53.7"	134°32'26.3"	9/7/2018	14:25:00	5.10	Dyke height
(h)	Hyogo, Minami Awa, Honjo river mouth	34°12'7"	134°43'41.9"	9/8/2018	08:30:00	3.77	Broken handrail
(i)	Hyogo, Minami Awa Fishing port	34°11'56.1"	134°47'43.5"	9/8/2018	09:20:00	3.06	Dyke height
(j)	Hyogo, Awa Nadakuroiwa	34°13'16.3"	134°49'44.1"	9/8/2018	09:58:00	6.37	Ground altitude
(k)	Hyogo, Awa Nadashirosaki	34°14'1.8"	134°51'15.7"	9/8/2018	10:05:00	5.77	Ground altitude
(l)	Hyogo, Kobe Meriken Park	34°40'53.2"	135°11'23.9"	9/8/2018	14:00:00	2.72	Ground altitude
(m)	Hyogo, Nishinomiya Yacht Harbour	34°42'37.3"	135°19'49.5"	9/8/2018	15:45:00	3.34	Debris
(n)	Hyogo, Nishinomiya Port Breakwater	34°42'28.5"	135°20'15.9"	9/8/2018	16:35:00	2.04	Dyke height
(o)	Hyogo, Nishinomiya Koshienhama	34°42'46.8"	135°21'12.7"	9/8/2018	17:10:00	4.91	Debris

the buildings looked robust against strong winds and exhibited no visible damage. However, we found evidence of wave overtopping in a coastal fence of 1.2 m high, which was smashed by high waves. The waves reached at least 2.7 m above the sea level (Fig. 7II). By using the GPS receivers, we measured elevations relative to TP of 4.14 and 6.03 m at Kainan and Saikazaki, respectively.

One of the coastal protection structures in Saikazaki seemed to be sufficiently strong against waves, but this area has two dyke layers, each with approximately 2-m parapets and armoring brocks supporting the first dyke. However, the parapet of the second dyke was smashed by overtopping waves, causing a deep hole due to scouring (Fig. 7III). The damage at this place was much severer than that at Kainan, suggesting that even neighboring coasts may have experienced different levels of wave impact by multiple factors such as the presence of offshore

Figure 5

Field survey at Nanko Bird Sanctuary and Sakai [locations (a, b) in Fig. 4III]. **I** Survey locations at the sanctuary, **II** trash accumulated over the main route, **III** sea dyke, **IV** scour behind the dyke due to wave overtopping, **V** damaged building near the dyke, **VI** difference in grass color demonstrating that seawater reached a height up to the withered grass and **VII** broken parapet at Sakai City outside (red dot: Sakai, blue dot: Nanko bird filed, yellow dot: Osaka)

breakwaters, wave directions, coastline, and local bathymetric features.

3.1.4 Locations (f) and (g): Anan and Minami Awa in Tokushima Prefecture

We visited a coastal village of Anan City, Tokushima (Fig. 8). This place is naturally protected by several islands. Although roofs and windows of a public sports hall were broken by strong winds (Fig. 8I), no serious damage was caused by coastal floods. A resident witnessed a quickly raising water level





Figure 6

Field survey at Rinku Park [location (c) in Fig. 4III]. **I** Park overview two days after Typhoon Jebi impact showing trash and a damaged roof. We measured the elevation of the ground where trash remained. **II** Inner and **III** outer protection layers of the park

during Typhoon Jebi. Although the waves did not exceed the dike, seawater intruded through a sewage pipe and partially flooded her house. A beach in Minami Awa Town located at the Southeast coast of Shikoku island has a sea dyke at approximately 4.7 m high from the ground, which effectively protected the village against high waves during Typhoon Jebi. According to another resident, high waves ran up and left many driftwoods on the sandy beach, but there was no considerable damage (Fig. 8II). Our measurements revealed that waves carried woods at least 5.1 m higher than TP.

3.1.5 Locations (h) to (k): Honjo river mouth, Minami Awa Fishing Port, Awa Nadakuroiwa and Awa Nadashirosaki in Awaji-shima island, Hyogo Prefecture

The Awaji-shima island is a remote island located next to Osaka Bay. We began the field survey at the Honjo river mouth located at the southern part of the island. There is a sandy beach separated from the Honjo river by a training wall (Fig. 9I). Several breakwaters parallel to the beach protect the coast. Trash, sand, and broken tree branches were on the beach, and the handrail of the training



Figure 7

Field survey at Wakayama [locations (d, e) in Fig. 4IV]. **I** Localization of Kainan and Saikazaki, **II** coastal fence smashed by high waves at Kainan, **III** broken parapet by overtopping waves at Saikazaki

wall had been apparently smashed by high waves and fell to the river (Fig. 9II). The direction of the fallen handrail suggests the primary direction of high waves, and the height from the local sea level to the top of the training wall was 3.77 m relative to TP, but we found no clear evidence of coastal inundation here.

The authors focused on the eastern coast of the island and carried out the field survey at several locations (Fig. 10I). The Minami Awa Fishing Port was protected by breakwaters with armor brocks on the sea side (Fig. 10II). Scattered fishing tools

indicated that the internal breakwater was overtopped. However, no considerable damage was observed at the port. Close to the fishing port, we found a road guardrail (reaching 6.37 m relative to TP) that was bent towards the land (Fig. 10III). Two large rubber fenders ($3 \text{ m} \times 1.3 \text{ m} \times 1.7 \text{ m}$) were washed away along with driftwoods by high waves and found on the coastal road at 5.77 m relative to TP. The wave force was strong enough to create a hole of $3.7 \text{ m} \times 2 \text{ m}$ on the wall behind the road (Fig. 10IV).

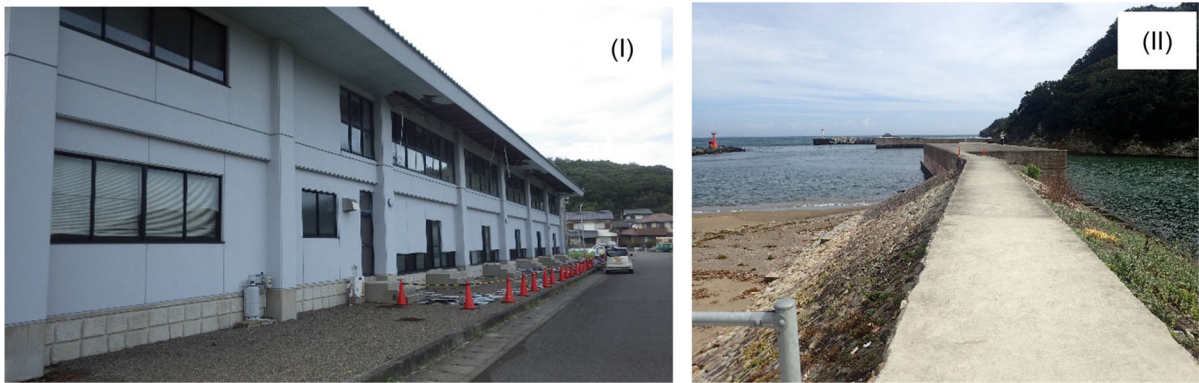


Figure 8

Field survey at Tokushima [locations (f, g) in Fig. 4IV]. **I** Damaged roof in a village from Anan, **II** high sea dyke at Minami Awa

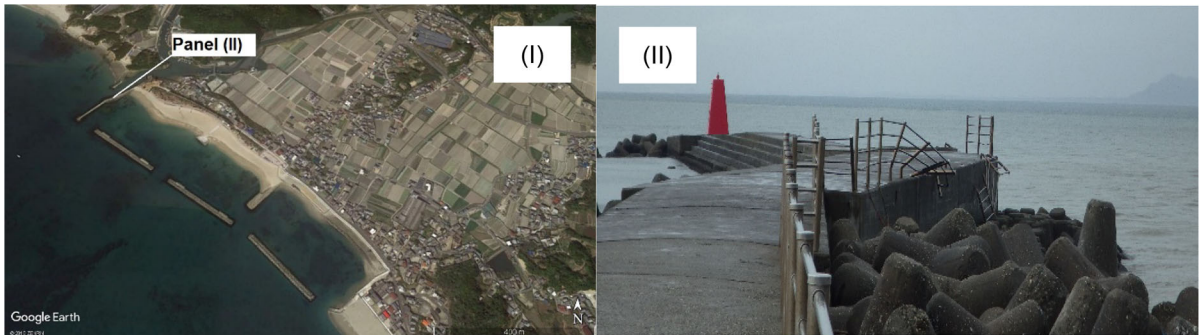


Figure 9

Field survey at Honjo river mouth [location (h) in Fig. 4IV]. **I** Location of training wall and **II** smashed handrail of the training wall

3.1.6 Locations (l) to (o): Kobe Meriken Park, Nishinomiya Yacht Harbor, Nishinomiya Port Breakwater and Koshienhama in Hyogo Prefecture

The Meriken Park in Kobe City was flooded due to high waves and storm surge, which overtopped the terrace of the park with elevation of 2.72 m relative to TP (Fig. 11I). Typhoon Jebi with strong winds of around 34.6 m/s (at Kobe airport) coincided with the flood tide period. Trash and debris had been already cleared when we visited the park 4 days after the typhoon (Fig. 11II). The building around the Meriken Park did not suffer considerable damage. We also investigated the Yacht Harbor in Nishinomiya, Hyogo Prefecture. The breakwater protected the harbor, preventing consequences from waves. However, there was a small damage on the wall at

approximately 3.34 m above the sea level (TP), as confirmed by fallen bricks (Fig. 11III). We observed the inland floodgate destroyed (Fig. 11IV) and a stranded large vessel on the top of the breakwater inside the Amagasaki Port, which is located next to the harbor (Fig. 11V). As this location belongs to the innermost part of the Osaka Bay, waves appear to be small under normal weather conditions. Therefore, the breakwater was constructed relatively low in height at only 2.04 m relative to TP. A high amount of trash was also accumulated on top of the breakwater, demonstrating wave overtopping (Fig. 11VI). An artificial beach in front of the residential area, named Koshienhama, was also damaged by high waves (Fig. 11VII). Based on the observed trash and driftwood left on top of the dyke, we confirmed that waves reached at least 4.91 m relative to TP, just



Figure 10

Field survey at eastern coast of Awaji-shima island [locations (i–k) in Fig. 4IV]. **I** Location of surveyed places, **II** armored breakwater at Minami Awa Fishing Port, **III** smashed guardrail at Awa Nadakuroiwa, **IV** rubber fenders found at Awa Nadashirosaki caused a large punching hole on a wall

below the crest of the concrete dyke that protects the populated hinterland.

3.2. Wind-Wave and Storm Surge Hindcasting

3.2.1 Wind and Pressure Fields

Before importing the wind speeds derived from the JMA GPVs as input to the hydrodynamic and wave model, we verified them with observed data from the stations. The observed data were measured at the relevant weather observation stations operated by the JMA (see Fig. 2). Figure 12 compares the observed and calculated wind speed at three stations, namely, Shionomisaki, Kansai airport, and Kobe airport. Despite the discrepancies between the measurements and estimations, the data from the GPVs show good agreement with the observed data at the peak time, with a slight underestimation (3–5 m/s). Air pressure measurements were taken from Shionomisaki, Tokushima, and Kobe stations due to the missing functions at some stations. The GPV air pressure data (988 hPa) at Shionomisaki retrieved a slight

underestimation from the maximum atmospheric pressure deficits (979 hPa). However, the estimated pressures at Tokushima and Kobe suitably agree with the measurements in terms of timing and magnitude (Fig. 13). The wind speed spatial distribution of the GPVs is shown in Fig. 14, which shows two snapshots when the typhoon (I) crossed the Kii Strait and (II) made landfall at Osaka. Both wind speed and air pressure from the GPV can be considered sufficiently reliable as external forces for storm surge and wave modelling.

3.2.2 Storm Surge Simulation

To investigate the effect from wave stresses transferring from the wave model during the coupling process, we ran the storm surge simulation in two scenarios: uncoupled and coupled with WAVE model. The scenario comparison shows that the water-level increase due to waves reached 11% of the total surge height in Osaka, while it was 8% and 9% in Tanowa and Kobe, respectively. These results suggest that wave-induced setup may have increased



Figure 11

Field survey at Kobe city [locations (I–o) in Fig. 4III]. **I** Kobe Meriken Park storm surge and high waves during Typhoon Jebi (rough sea screenshot from online live camera at 14:17, September 4, 2018, Japan Standard Time) (<https://www.youtube.com/watch?v=lCupBcgCuO8>), **II** situation after 4 days of the typhoon at Kobe Meriken Park, **III** fallen bricks at Nishinomiya Yacht Harbor, **IV** destroyed inland floodgate at Amagasaki Port, **V** stranded large vessel at Amagasaki Port, **VI** trash gathered behind breakwater, **VII** Koshienhama Artificial Beach, where wave overtopping was confirmed

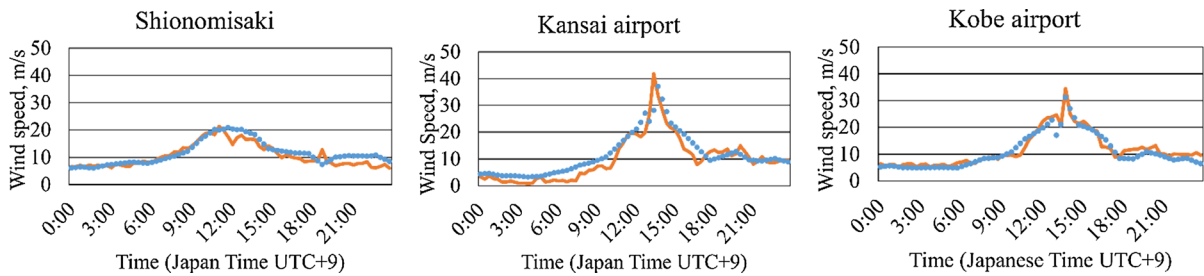


Figure 12

Comparison between wind speed obtained from the JMA mesoscale spectral model (blue dotted line) and observed data (orange solid line) on 4 September 2018 (time in Japan Standard Time, UTC + 9)

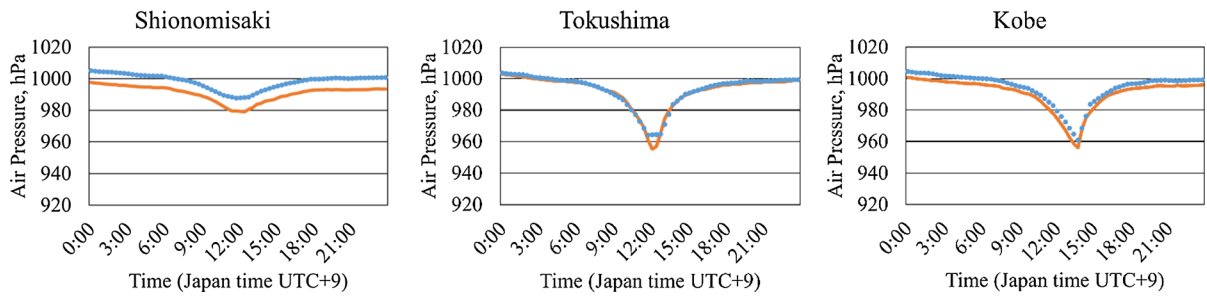


Figure 13

Comparison between air pressure obtained from the JMA mesoscale spectral model (blue dotted line) and observed data (orange solid line) on 4 September 2018 (time in Japan Standard Time, UTC + 9)

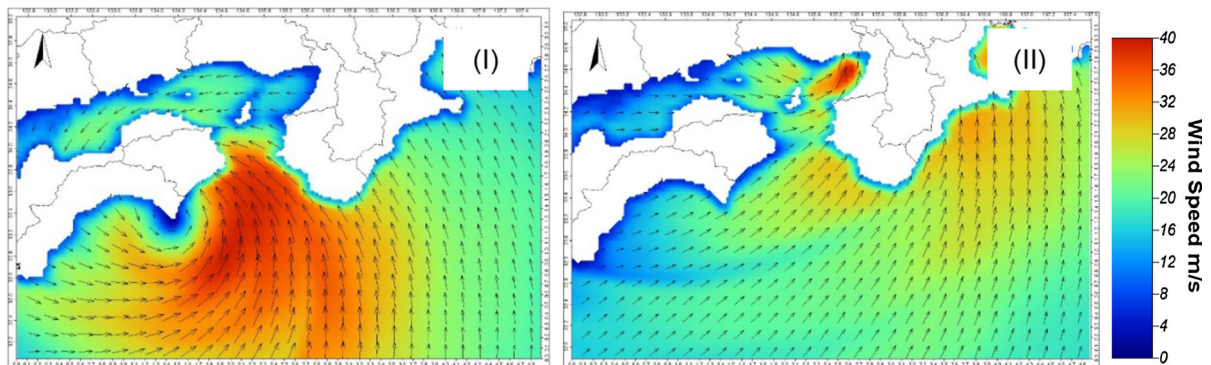


Figure 14

Wind field distribution during Typhoon Jebi passage **I** over Kii Strait on September 4, 2018 at 11:00 and **II** inside Osaka Bay at 14:00 (Japan Standard Time, UTC + 9)

the water level in Osaka Bay by approximately 10%. Results from numerical simulations of the surge component caused by Jebi and using the coupled model are compared with real data at Tanowa, Kobe, and Osaka respectively in Fig. 15. The increasing water level during the passage of Jebi is suitably reflected by Delft3D-FLOW model (maximum difference was about 10% at Tanowa, RMS values of 0.23, 0.21, and 0.18 at Osaka, Kobe, and Tanowa, respectively). Figure 15 shows that the simulated surge height reached up to 1.75 m in Osaka, while the observed data was 1.61 m from the tidal gauge. This small overestimation can be partially attributed to the land-boundary condition in the model, which does not consider overflow, whereas coastal floods took place in some port areas (Takabatake et al. 2018). The water surface elevation at Osaka started increasing at 13:00 and reached its peak at 15:00, while 47.4 m/s of maximum wind speed was recorded in

Osaka at 14:10. Thus, there is about a 1-h lag between the growth of wind speed and water level. Similar lag times were observed at Tanowa and Kobe. The spatial distribution of the maximum surge level when Jebi crossed the Kii strait and hit land at Osaka are shown in Fig. 16.

3.2.3 Wind-Wave Simulation

We also ran the wave model in two cases, namely, with and without transfer of water level from the flow model, to investigate the effect of the storm surge on significant wave height. This comparison revealed that at Kaiyo Tokushima and Shionomisaki, where the water depth is large, there is no remarkable difference in wave heights for both cases. By considering this interaction, however, a slightly higher wave height is observed at Kobe and Komatsujima (0.08 m and 0.04 m, respectively) because the

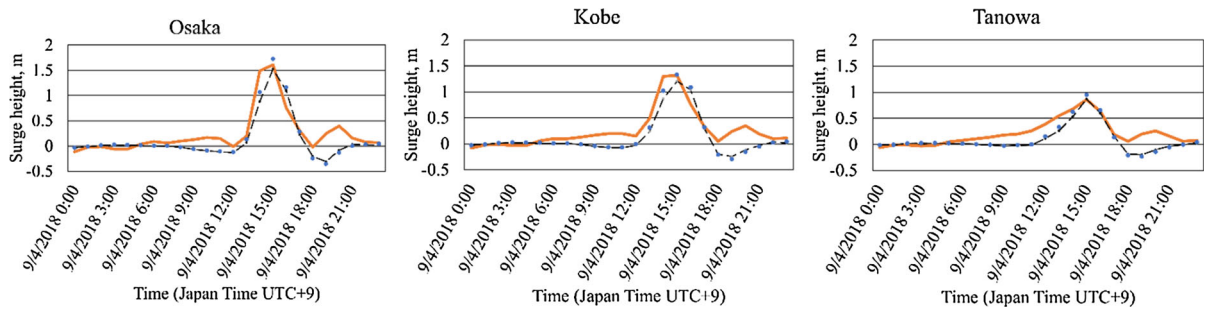


Figure 15

Comparison of calculated surge level with flow–wave interaction (blue dotted line), no interaction with wave (black dash line), and observed values (orange solid line) during Jebi passage

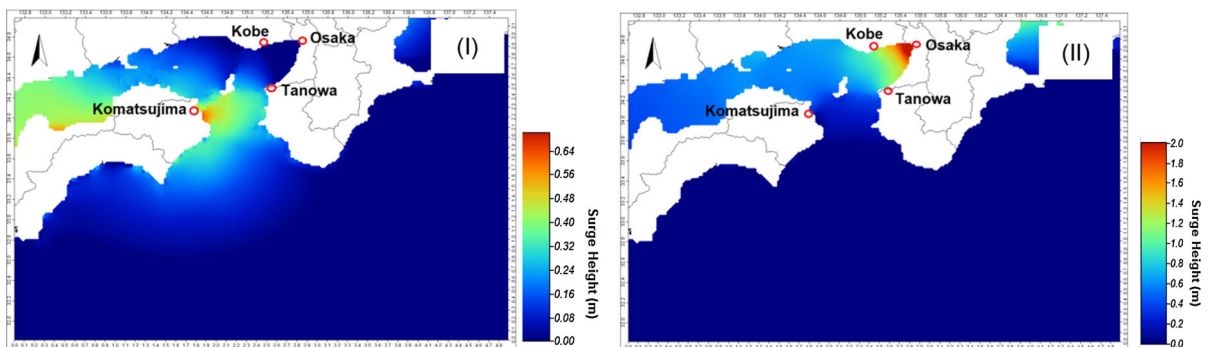


Figure 16

Storm surge distribution during Typhoon Jebi passage **I** over Kii Strait on September 4, 2018 at 12:00 and **II** inside Osaka Bay at 15:00 (Japan Standard Time, UTC + 9)

depth-limited condition is relaxed due to the increased water depth. Hereafter, the wave simulation coupled with the flow simulation is considered to account for the influence of the wave–flow interaction. Figure 17 shows the simulation accuracy by comparing the estimated significant wave height with data measured from NOWPHAS, showing a reasonable agreement especially at the peak values at all stations. The model underestimates the significant wave height by up to 2.7 m at the Kaiyo Tokushima buoy likely by the difference in wind speed. The measured wind speed at Murotomisaki station (Fig. 2) near Kaiyo Tokushima was 47.7 m/s, which was much higher than the 30.3 m/s obtained from the GPV model. The simulation results also underestimated the real data at Shionomisaki and Kobe, while a slight overestimation (0.1 m) was found at Komatsujima. The mesoscale model has a limitation to

estimate the wind field, particularly near the center of typhoons (Tanemoto and Ishihara 2013, 2015). As the Murotomisaki station and Kaiyo Tokushima buoy were closer to the Jebi track than other stations, the wave height tends to be underestimated. Simulation waves at Tokushima-Komatsujima and Kobe port show better RMS values (0.62 m and 0.37 m, respectively) than the other two offshore stations, Kaiyo-Tokushima and Shionomisaki (2.98 and 2.04, respectively).

Figure 18I shows that the maximum significant wave height was nearly 13 m in the strait between Shikoku and Honshu island when the typhoon made landfall at the coast of the Tokushima Prefecture. The east coast of Shikoku island suffered the highest wave about 2 h before the west coast of Wakayama Prefecture was affected. The simulation also shows

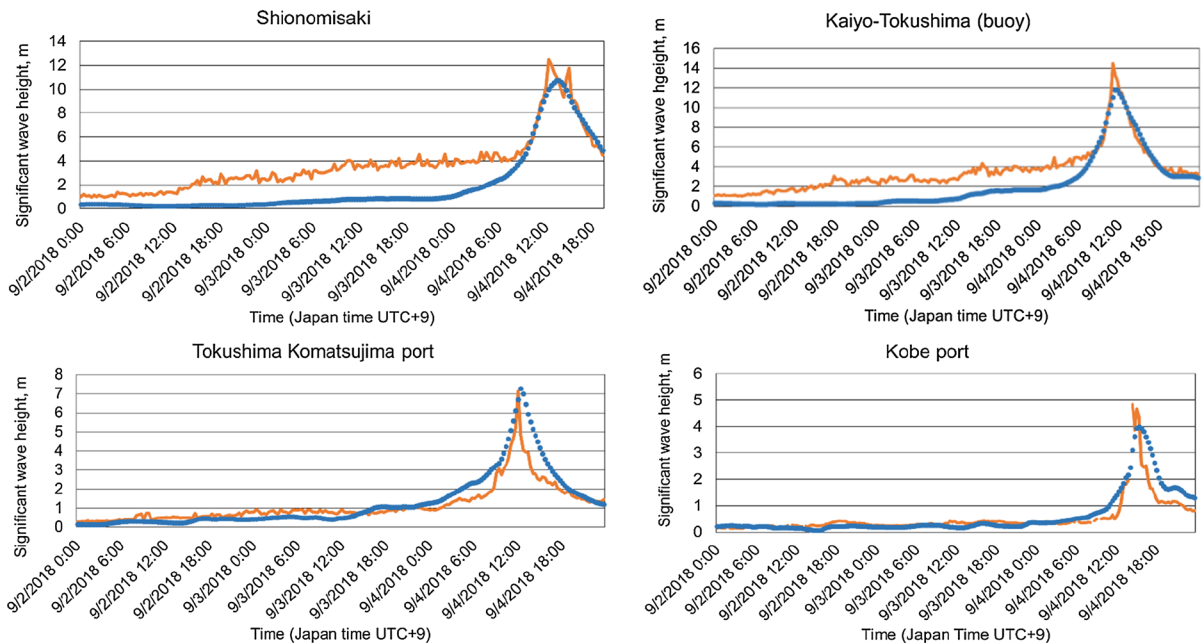


Figure 17

Significant wave height obtained from our surge-wave model (blue dotted line) and observed data (orange solid line). Time is expressed in Japan Standard Time, UTC + 9

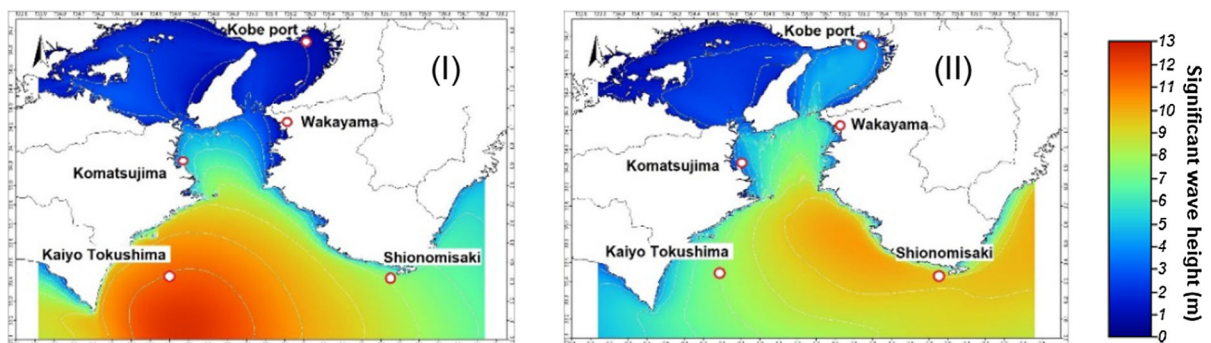


Figure 18

Significant wave height distribution during Typhoon Jebi passage **I** over Kii Strait on September 4, 2018 at 11:00 and **II** inside Osaka Bay at 14:00 (Japan Standard Time, UTC + 9)

that waves up to 4 m high were generated near Osaka and Kobe (Fig. 18II).

It should be noted that wave height tends to be underestimated when the typhoon moved far off the coast. For example, recorded data at Shionomisaki and Kaiyo-Tokushima indicate that wave height has already reached 2–4 m even a few days before the arrival of the typhoon. This is probably because of the

propagation of swell, prior to the occurrence of locally generated wind waves. The larger domain, shown in Fig. 2, is large enough to reproduce the wind-generated waves, but may not be sufficient to cover the swell that travels from far off towards the coast. Therefore, we only focused on the reproducibility of wave height during the peak of the typhoon. In this sense, the model is accurate, as the

RMS values at Kaiyo-Tokushima and Shionomisaki around the peak (when the fact of swell is not captured) are 0.75 and 0.84, respectively.

4. Discussion

Japan has an advanced wave monitoring network, with monitoring sensors deployed at over 70 locations along the coastline. Nevertheless, not many wave monitoring stations were present to evaluate the wave records during the passage of Typhoon Jebi. We have demonstrated that at locations with limited wave data, hindcasting using numerical models can be reliable to evaluate the extent of waves produced by Jebi. Besides high waves, substantial storm surge was also generated by strong winds reaching speeds above 35 m/s and leading to abnormal sea levels during Typhoon Jebi. For example, the Kansai airport was flooded and its operation was interrupted for a prolonged period (about 2 days), notably affecting the socioeconomic conditions in the affected region.

According to the simulation results, the highest waves reached 4.2 and 3.1 m at Kansai International Airport and Rinku Park (opposite shore of the airport), respectively. The airport has a surrounding revetment 4.4–5.9 m high above the chart datum level (MLIT 2018). The tidal graph at the nearest station of Tannowa shows that the anomaly due to storm surge reached only 1.2 m, as presented in Fig. 19. Hence, the combined impact of high waves and storm surge appears to be responsible for the flooding at the airport.

Our field survey also confirmed that the heights of wave overtopping reached at least 8.0 and 6.8 m above the sea level at two locations in Wakayama prefecture, namely, Saikazaki and Kainan, respectively. The estimation with the wind-wave model also shows wave heights of 6.8 m in Saikazaki. The tide data at the adjacent station in Gobo showed a tidal anomaly of 1.7 m. Although the storm surge was significant, it did not reach extreme severity. Hence, the destruction of the dykes in the coasts, as shown in Fig. 7, should be investigated by considering the combination of high waves and storm surge.

Results from sea level data analyses are shown in Fig. 19. Among the 12 tide gauge stations examined

in this study, the SA and SD were in the ranges of 0.3–2.7 m and 0.43–1.3 days, respectively. The highest SA and SD were observed in Osaka (2.7 m) and Kobe (1.3 days), respectively. The two locations experiencing the highest SA were Kobe and Osaka, located at the end of Osaka Bay. This can be likely due to the funneling of the storm surge at the end of the bay. Stations located very close (< 50 km) to the typhoon trajectory (e.g., Murotomisaki, Komatsujima, Sumoto, and Tannowa) recorded SAs above 1 m, whereas farther locations (e.g., Kushimoto, Kumano, Tosashimizu, and Takamatsu) experienced SAs below 1 m (Fig. 3). The only exception is Nagoya, which registered a SA of 1.4 m despite of being located at approximately 80 km from the typhoon trajectory.

Table 2 shows the wave heights (derived from simulation results) and storm surge levels (derived from sea level analyses) that demonstrate the varying wave impact depending on the location. The lowest wave–storm surge ratio was 0.8, obtained at Osaka, whereas the highest was 15.2 at Kushimoto. The ratio is particularly high at Kushimoto, Murotomisaki, and Gobo, places that face directly to the Pacific Ocean (Fig. 3). This ratio can serve as indicator to determine the extent of wave impact at a particular site compared to the storm surge. It is reasonable to find the lowest value at Osaka, because the innermost part of the bay is naturally protected from high waves, but the water depth tends to be shallow, thus amplifying storm surges. Interestingly, however, the ratio at Kobe jumps up to 2.0, although the city is close to Osaka. This is probably because the wind direction and speed caused by Typhoon Jebi were more adverse in Kobe than in Osaka (Fig. 14II). The storm surge level of up to 1.7 m at Kobe was considerable. However, storm surge alone may not have accounted for the destruction of the inland floodgate and the stranded large vessel on the breakwater, as shown in Fig. 11 IV, V, respectively. It appears that the bay area from Osaka to Kobe, located in the semi-enclosed Osaka Bay, has been historically considered as a tranquil environment without high waves. However, Typhoon Jebi has reminded us that winds caused by a typhoon traveling into an adverse trajectory can produce high waves along with storm surges, which might substantially damage waterfront areas.

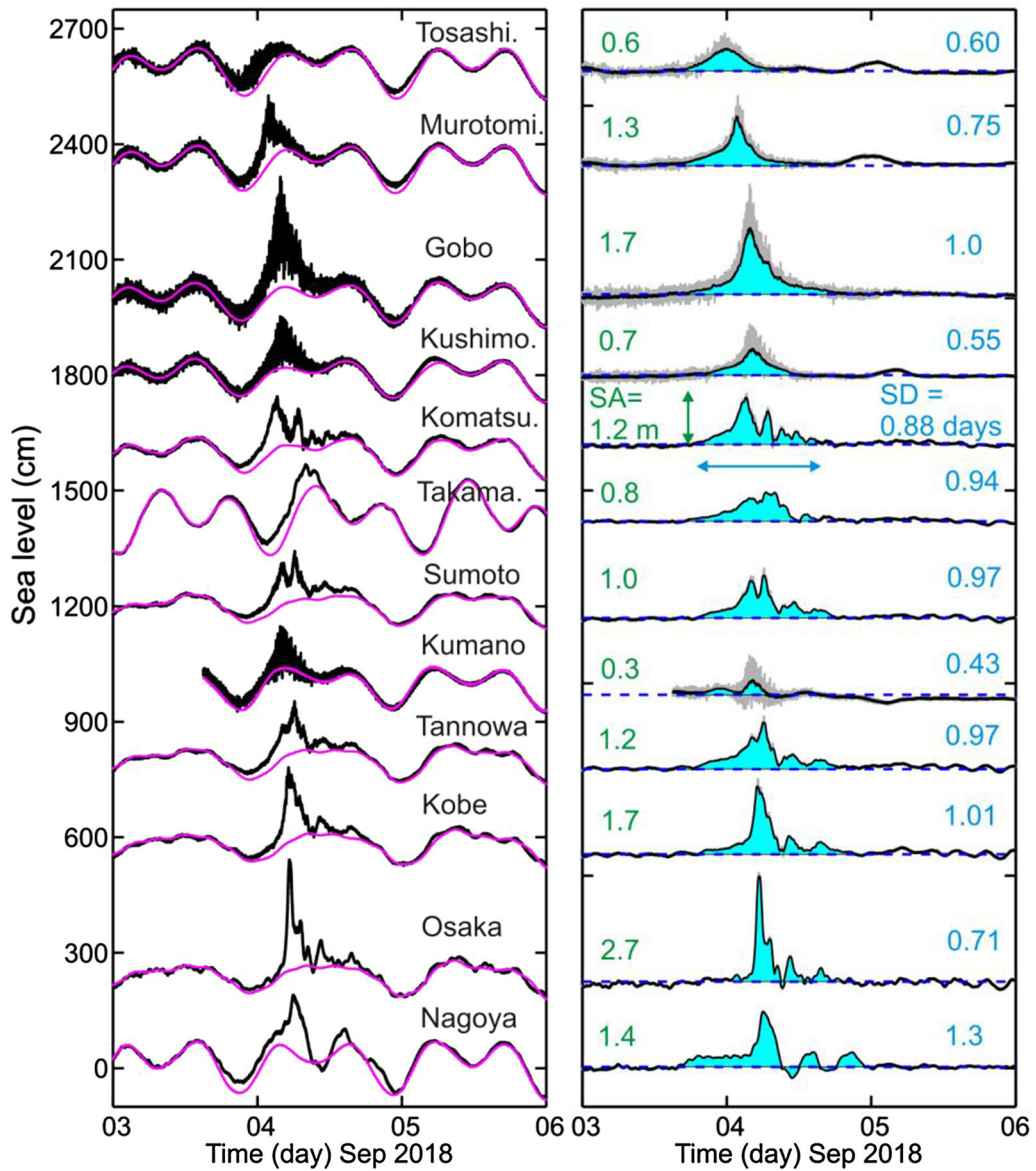


Figure 19

Sea level in September 2018 affected by Typhoon Jebi based on analyses of tide gauge data. **a** Original tide gauge records (black) and tide prediction (pink). **b** SA and SD at different tide gauge stations (black solid lines, 15-min average waveforms to remove wave effects)

Figure 20 shows the power spectrum of component waves derived using the fast Fourier transform over the original tidal data recorded at a 15-s interval. Osaka and Kushimoto were selected because Table 2 shows the maximum and minimum wave height/storm surge ratio at these locations. Figure 20 enables an in-depth analysis in terms of the frequency domain. The data at Kushimoto show that a peak

appears around 70 s (0.014 Hz), which is within the typical range of infragravity waves. However, data at Osaka do not show any particular increase during the same period. The power spectrum at Kushimoto is greater than that at Osaka for high frequency ($> 10^{-2}$ Hz), demonstrating the predominance of wind waves at Kushimoto. This is also evident from Fig. 19, where noisy fluctuations in Kushimoto appear.

Table 2

Wave height and storm surge level at 8 locations in Kii Strait and Osaka Bay and the wave/surge ratios caused by the 2018 Typhoon Jebi

Location	Wave height (m)	Storm surge (m)	Ratio wave height/storm surge
Osaka	2.2	2.7	0.8
Kobe	3.5	1.7	2.0
Tannowa	2.2	1.2	1.8
Sumoto	3.0	1.0	3.0
Komatsujima	3.5	1.2	2.9
Gobo	8.0	1.7	4.7
Kushimoto	10.7	0.7	15.2
Murotomisaki	9.9	1.3	7.6

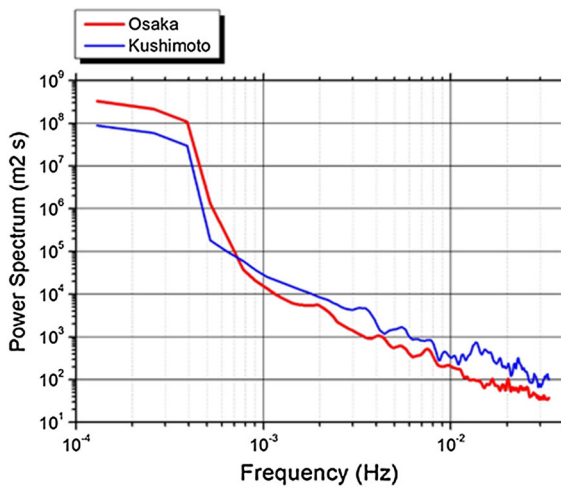


Figure 20

Power spectrum of component waves during 12 h including the arrival time of Typhoon Jebi

However, the power spectrum at Osaka is larger than at Kushimoto in the range of below 7×10^{-4} Hz (period of over 24 min), most likely resulting from the storm surge dominance at Osaka.

In addition to those floods induced by storm surge and high waves, there is another non-negligible mechanism, often called meteorological tsunami or meteo-tsunami, that excites sea level oscillations as long waves. This mechanism is related to atmospheric forcing, such as gravity waves, pressure jumps, frontal passages, and squalls, that generates waves with similar periods in typical seismic tsunami waves (Rabinovich and Monserrat 1996, 1998; Monserrat et al. 2006). The low-pressure system of a

typhoon that propagates over the open ocean may also amplify water levels near the coast through specific resonance mechanisms (i.e., Proudman, Greenspan, or shelf resonance) (Monserrat et al. 2006). For example, a very strong seiche-type oscillation, locally known as *abiki*, was observed in Nagasaki Bay, Japan, during the event of 31 March 1979, causing an abnormal tidal fluctuation of 2.78 m excited by a moving low-pressure system (Hibiya and Kajiuura 1982). Although we did not investigate this phenomenon, it is possible that the present coastal flood might have been partially exacerbated by this kind of resonance mechanisms in Osaka Bay.

5. Conclusion

Typhoon Jebi has been one of the strongest typhoons over the past 25 years to hit Osaka Bay and Kansai area, leaving substantial human and property losses. During our field survey in the typhoon aftermath, we found damaged coastal protection structures at many sites. Damage was most likely caused by storm surge in Osaka. However, those caused by high waves were more frequent in other prefectures such as Wakayama, Tokushima and Hyogo. The tidal anomaly due to the storm surge was analyzed by using JMA short-interval tidal data. Among the 12 evaluated gauge stations, the highest storm surge of 2.7 m occurred in Osaka. Wind waves were also estimated using the SWAN model with data of wind and pressure fields retrieved from the JMA GPVs. The estimated waves were sufficiently accurate when compared to observed data at four wave monitoring stations. Wave heights reached nearly 12.0 and 10.7 m at Tokushima and Shionomisaki, respectively. Waves were smaller in the innermost part of Osaka Bay, reaching only 2.2 m in Osaka. By performing the storm surge-wave coupled model, we also found that the radiation stresses play an important role to increase storm surge, while influence from the storm surge simulation to the wave simulation is relatively minor. Based on our estimations, we calculated the ratio of wave height to storm surge to examine the extent of wave impact compared to that of storm surge. The ratio was the lowest at Osaka (0.8), demonstrating that storm surge played more important role than impact of high wave for the coastal damage in Osaka. On the other

hand, wave effect was predominant in Kobe, close to Osaka and situated within the bay, exhibited a ratio of 2.0 which is more than double of that in Osaka. Generally, the combination of the storm surge and the waves were responsible for the large coastal damages inside the bay. Near Kobe, the height of the breakwater, on which a large vessel stranded, was remarkably low (1.7 m above the sea level) compared to the maximum wave height of nearly 4 m that occurred there. This discrepancy between the design height of breakwaters and actual waves during Typhoon Jebi demonstrates that the effect of waves has been underestimated compared to that of storm surge.

Acknowledgements

We are grateful to the Japan Meteorological Agency for providing sea level data for this study (<https://www.jma.go.jp/jma/indexe.html>) as well as hourly wind field data. This research was funded through the Grant for HT, Tokyo Institute of Technology (Japan Society for the Promotion of Science, 16KK0121 and 19K04964). MH was also funded by the Brunel University London through the Brunel Research Initiative and Enterprise Fund 2017/18 (BUL BRIEF) and the Great Britain Sasakawa Foundation Grant number 5542. LTA appreciates the scholarship from the JICA AUN/SEED-Net.

Publisher's Note Springer Nature remains neutral with regard to jurisdictional claims in published maps and institutional affiliations.

REFERENCES

- Booij, N., Ris, R. C., & Holthuijsen, L. H. (1999). A third-generation wave model for coastal regions I. Model description and validation. *Journal of Geophysical Research*, 104(4), 7649–7666.
- Bricker, J., Takagi, H., Mas, E., Kure, S., Adriano, B., & Yi, C., et al. (2014). Spatial variation of damage due to storm surge and waves during Typhoon Haiyan in the Philippines. *Journal of Japan Society of Civil Engineers*, 70(2), I_231–I_235.
- Chen, Q., Wang, L., & Zhao, H. (2008). *An integrated surge and wave modeling system for Northern Gulf of Mexico: simulations for Hurricanes Katrina and Ivan* (pp. 1072–1084). Proceedings of International Conference on Coast Engineering: ASCE.
- Fire and Disaster Management Agency. (2018). Damages by Typhoon No. 21 in 2018 and the response of fire and disaster management agency. <http://www.fdma.go.jp/bn/5088fc7540585e7232370c8db10e55e8b1c909ae.pdf>. Accessed 19 Jan 2019
- Fritz, H. M., Blount, C., Sokoloski, R., Singleton, J., Fuggle, A., McAdoo, B. G., et al. (2007). Hurricane Katrina storm surge distribution and field observations on the Mississippi Barrier Islands. *Estuarine, Coastal and Shelf Science*, 74(2007), 12–20.
- Funakoshi, Y., Hagen, S. C., & Bacopoulos, P. (2008). Coupling of hydrodynamic and wave models: case study for Hurricane Floyd (1999) Hindcast. *Journal Of Waterway, Port, Coastal, And Ocean Engineering*, 15, 8. [https://doi.org/10.1061/\(asce\)0733-950x\(2008\)134:6\(321\)](https://doi.org/10.1061/(asce)0733-950x(2008)134:6(321)).
- Grinsted, A. (2008). Tidal fitting toolbox. https://uk.mathworks.com/matlabcentral/675fileexchange/19099-tidal-fitting-toolbox?focused=3854016&tab=function&s_tid=gn_loc_drop. Accessed 29 March 2018.
- Heidarzadeh, M., Teeuw, R., Day, S., & Solana, C. (2018). Storm wave runups and sea level variations for the September 2017 Hurricane Maria along the coast of Dominica, eastern Caribbean Sea: evidence from field surveys and sea level data analysis. *Coastal Engineering Journal*. <https://doi.org/10.1080/21664250.2018.1546269>.
- Hibiya, T., & Kajiura, K. (1982). Origin of 'Abiki' phenomenon (kind of seiches) in Nagasaki Bay. *Journal of the Oceanographical Society of Japan*, 38, 172–182.
- Japan Meteorological Agency. The numerical forecast data/observation data. <http://database.rish.kyoto-u.ac.jp/arch/jmadata/data/>. Accessed 20 Nov 2018.
- Japan Meteorological Agency. (2018). Wind storm and storm surges by Typhoon No. 21. <https://www.data.jma.go.jp/obd/stats/data/bosai/report/2018/20180911/20180911.html>. Accessed 19 Jan 2019.
- Japan Oceanographic Data Center (JODC). http://jdos1.jodc.go.jp/vpage/depth500_file.html. Accessed 20 Nov 2018.
- Japan Times News. (2018). Typhoon Jebi, most powerful to hit Japan in 25 years, leaves trail of destruction in Kansai region. <https://www.japantimes.co.jp/news/2018/09/04/national/strong-typhoon-poised-make-landfall-shikoku-kii-peninsula-afternoon/#.XKHtopgzaUk>
- Hydrographic and Oceanographic Department. https://www1.kaiho.mlit.go.jp/KANKYO/TIDE/real_time_tide/sel/index_e.htm.
- Longuet-Higgins, M. S., & Stewart, R. W. (1960). Changes in the form of short gravity waves on long waves and tidal currents. *Journal of Fluid Mechanics*, 8, 565–583.
- Longuet-Higgins, M. S., & Stewart, R. W. (1962). Radiation stress and mass transport in gravity waves with application to surf beat. *Journal of Fluid Mechanics*, 13, 481–504.
- Mikami, T., Shibayama, T., Takagi, H., Matsumaru, R., Esteban, M., & Thao, N. D., et al. (2016). Storm surge heights and damage caused by the 2013 Typhoon Haiyan along the Leyte Gulf Coast. *Coastal Engineering Journal*, 58(1), 1640005.
- MLIT. (2018). Kinki Regional Development Bureau, Annual Research Presentation. <https://www.kkr.mlit.go.jp/plan/happyou/thesises/2018/pdf04/ino1-14.pdf>
- Monserrat, S., Vilibić, I., & Rabinovich, A. B. (2006). Meteor-sunamis: Atmospherically induced destructive ocean waves in the tsunami frequency band. *Natural Hazards and Earth Systems Sciences*, 6, 1035–1051.
- Nationwide Ocean Wave information network for Ports and Harbours (NOWPHAS). <https://nowphas.mlit.go.jp/eng/>. Accessed 25 Nov 2018.

- NDRRMC. (2014). Effects of Typhoon “YOLANDA” (HAIYAN), SitRep No.106.
- Rabinovich, A. B., & Monserrat, S. (1996). Meteorological tsunamis near the Balearic and Kuril Islands: Descriptive and statistical analysis. *Natural Hazards*, 13(1), 55–90.
- Rabinovich, A. B., & Monserrat, S. (1998). Generation of meteorological tsunamis (large amplitude seiches) near the Balearic and Kuril Islands. *Natural Hazards*, 18(1), 27–55.
- Roeber, V., & Bricker, J. D. (2015). Destructive tsunami-like wave generated by surf beat over a coral reef during Typhoon Haiyan. *Nature Communications* 6:7854. <https://doi.org/10.1038/ncomms8854>, www.nature.com/naturecommunications.
- Saito, K., Fujita, Ta, Yamada, Y., Ishida, J., Kumagai, Y., Aranami, K., et al. (2006). The operational JMA nonhydrostatic model. *Monthly Weather Review*, 134, 1266–1298.
- Takabatake, T., Mäll, M., Esteban, M., Nakamura, R., Kyaw, T. O., Ishii, H., et al. (2018). Field survey of 2018 Typhoon Jebi in Japan: Lessons for disaster risk management”. *Geosciences*, 8, 412. <https://doi.org/10.3390/geosciences8110412>.
- Takagi H., Anh L. T., & Thao N. D. (2017). 1997 Typhoon Linda Storm Surge and People’s Awareness 20 Years Later: Uninvestigated Worst Storm Event in the Mekong Delta. *Natural Hazards Earth System Science Discussion, European Geosciences Union*
- Takagi, H., & Esteban, M. (2016). Statistics of tropical cyclone landfalls in the Philippines -Unusual Characteristics of 2013 Typhoon Haiyan. *Natural Hazards*, 80(1), 211–222.
- Takagi, H., Li, S., de Leon, M., Esteban, M., Mikami, T., Matsumaru, R., et al. (2016). Storm surge and evacuation in urban areas during the peak of a storm. *Coastal Engineering*, 108, 1–9.
- Takagi, H., Pratama, M. B., Kurobe, S., Esteban, M., Aránguiz, R., & Ke, B. (2019). Analysis of generation and arrival time of landslide tsunami to Palu City due to the 2018 Sulawesi earthquake. *Landslides*, 16(5), 983–991.
- Takagi, H., Xiong, Y., & Furukawa, F. (2018). Track analysis and storm surge investigation of 2017 Typhoon Hato: were the warning signals issued in Macau and Hong Kong timed appropriately?. *Georisk*, 12(4), 297–307.
- Tanemoto, J., & Ishihara, T. (2013): Prediction of tropical cyclone induced wind field by using mesoscale model and JMA best track. In: *The Eighth Asia-Pacific Conference on Wind Engineering, December 10–14, 2013*, Chennai, India.
- Tanemoto, J., & Ishihara, T. (2015). Numerical study of wind wave and swell by using wave prediction models and combined wind fields. In: *EWEA Offshore 2015- Copenhagen-10-12 March 2015*.
- Tsuji, H., Miyagawa, K., Yamaguchi, K., Yahagi, T., Oshima, K., Yamao, H., et al. (2013). Modernization of GEONET from GPS to GNSS. *Bulletin of the Geospatial Information Authority of Japan*, 61, 9–20.
- Xie, L., Liu, H., & Peng, M. (2008). The effect of wave–current interactions on the storm surge and inundation in Charleston Harbor during Hurricane Hugo 1989. *Ocean Modelling*, 20, 252–269.

(Received April 8, 2019, revised July 30, 2019, accepted July 31, 2019, Published online August 8, 2019)